Curvature of the Galaxy Brightness Profile for Structural Analysis

Workshop Galaxies in Porto Alegre

Geferson Lucatelli, Fabricio Ferrari

UFRGS - Porto Alegre, December 19, 2018

Universidade Federal do Rio Grande

Instituto de Matemática, Estatística e Física

Summary

Introduction

$$\text{morphology} \quad \rightarrow \quad \begin{cases} \text{photometry (parametric)} \\ \text{morphometry (non-parametric)} \end{cases}$$

- parametric: profile fitting (e.g. Sérsic law) (Caon et al., 1993; de Souza et al., 2004; Erwin, 2015; Gadotti, 2008; Peng et al., 2002; Simard et al., 2011; Sérsic, 1963), , ellipse fitting, (Cabrera-Lavers and Garzón, 2004; Erwin and Sparke, 2003; Gadotti et al., 2007; Jungwiert et al., 1997; Laurikainen et al., 2005), ...
- non-parametric: CASGM-$H\sigma_{\psi}\varkappa$ (Abraham et al., 1994; Bershady et al., 2000; Conselice et al., 2000; Ferrari et al., 2015; Kent, 1985));

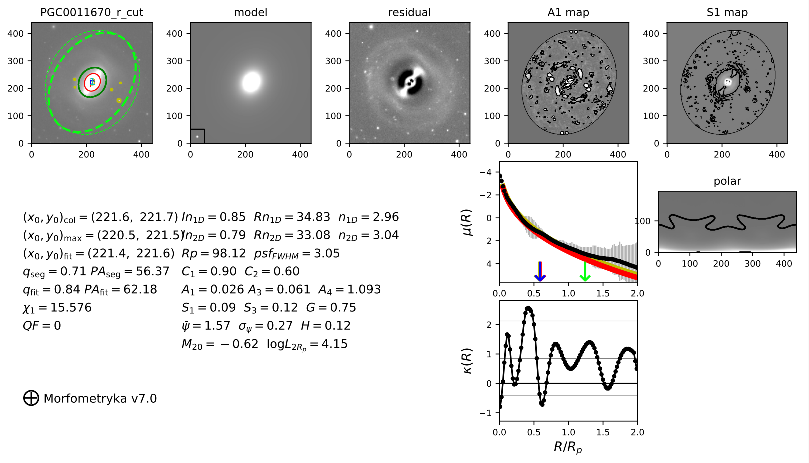

Figure 1: Example for NGC 1211.

Curvature

What about a non-parametric way for multicomponent/structural analysis?

Curvature

MNRAS **000**, 000–000 (2018?) Preprint December 13, 2018 Compiled using MNRAS LaTeX style file v3.0

Curvature of the Galaxy Brightness Profile for Structural Analysis

Geferson Lucatelli,[1]⋆ Fabricio Ferrari,[1]†
[1]*Instituto de Matemática Estatística e Física – IMEF, Universidade Federal do Rio Grande – FURG, Rio Grande, RS, Brazil.*

Accepted XXX. Received YYY; in original form ZZZ

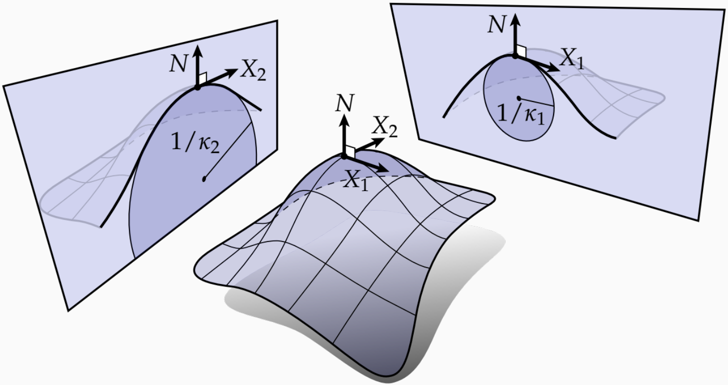

Figure 2: Adapted from Crane et al. (2013)

What:

We apply the curvature on the galaxy profile in order to study how each part of it changes along radius.

Objectives:

Identify and characterise galaxy multicomponents.

- normalizations for enhancing smooth structures and preserve curvature's definition:

$$\nu(R) \equiv \frac{\log[I(R)] - \min(\log I)}{\max(\log I) - \min(\log I)}, \qquad \chi = \frac{R}{2R_p} \tag{1}$$

- why $\log I$?

Because the curvature of a disk in log space is ZERO!!

Normalized curvature $\widetilde{\varkappa}$:

$$\widetilde{\varkappa}(R) = \frac{\dfrac{d^2\nu(R)}{d\chi^2}}{\left[1 + \left(\dfrac{d\nu(R)}{d\chi}\right)^2\right]^{3/2}} = \frac{4R_p^2\dfrac{d^2\nu(R)}{dR^2}}{\left[1 + 4R_p^2\left(\dfrac{d\nu(R)}{dR}\right)^2\right]^{3/2}}. \qquad \text{(continuous)} \quad (2)$$

$$\widetilde{\varkappa} = \frac{\delta\chi_i\delta^2\nu_i - \delta\nu_i\delta^2\chi_i}{\left(\delta\chi_i^2 + \delta\nu_i^2\right)^{3/2}}. \qquad \text{(discrete)} \quad (3)$$

Curvature for a single Sérsic Law

$$\nu(R) = 1 - \left(\frac{R}{2R_p}\right)^{1/n}, \qquad \widetilde{\varkappa}(R) = \frac{\frac{n-1}{n^2}\left(\frac{R}{2R_p}\right)^{\frac{1-2n}{n}}}{\left[1 + \frac{1}{n^2}\left(\frac{R}{2R_p}\right)^{\frac{2-2n}{n}}\right]^{3/2}}. \tag{4}$$

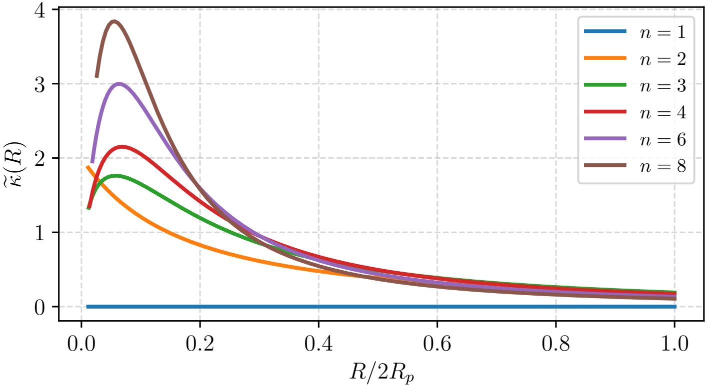

- adaptive Gaussian filter:

$$G(R) = \frac{1}{\sigma\sqrt{2\pi}} e^{-\frac{(R-R_0)^2}{2\sigma^2}} \tag{5}$$

with σ-variable given by

$$\sigma = (\sigma_{\max} - \sigma_{\min}) \frac{R}{2R_p} + \sigma_{\min}; \tag{6}$$

- generally $\sigma_{\min} \lesssim 2$ and $\sigma_{\max} \sim 0.1 \times (2R_p)$.

Example

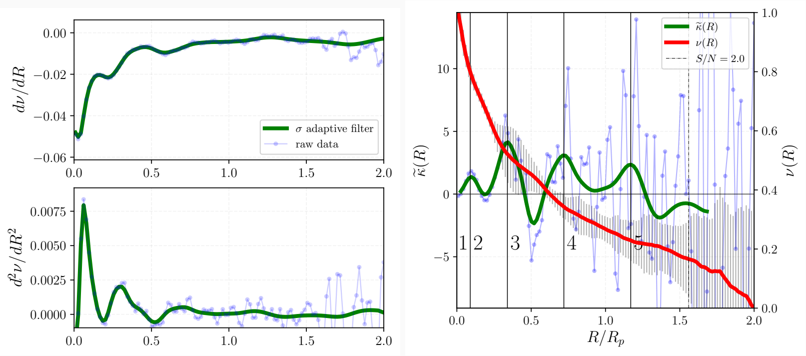

Figure 4: Example for galaxy NGC 1211 (r-band) from EFIGI sample.

Reference Example: NGC 1211 – (R)SB(r)0/a

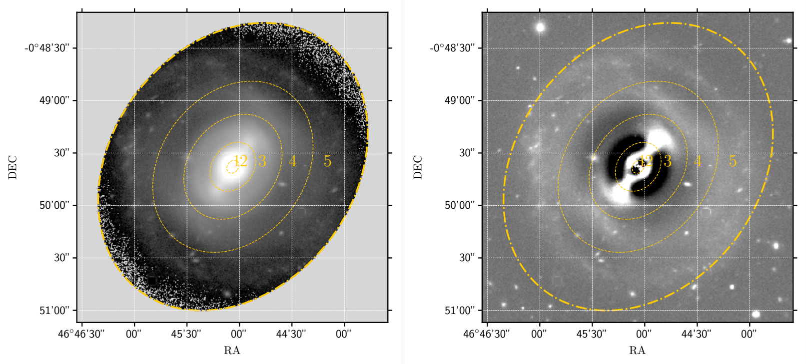

Figure 5: Ellipses gathered by the peaks in the curvature.

Some results until now...

NGC 936 – SB0

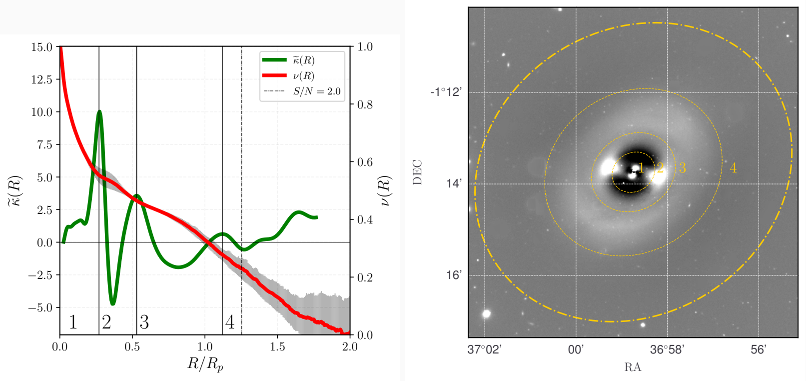

Figure 6: NGC 936

NGC 4267 – S0

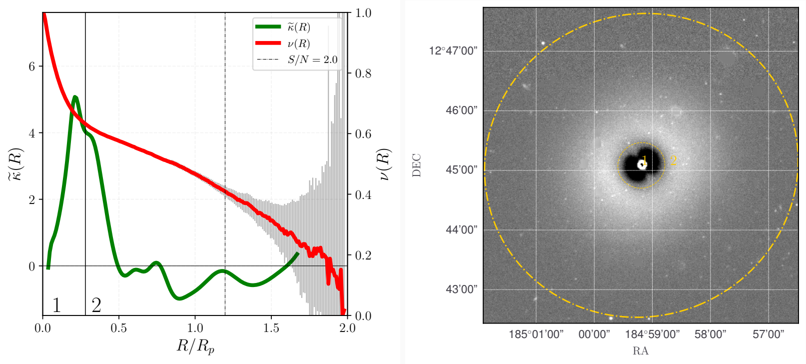

FIGURE 7: NGC 4267

NGC 7723 – SB(r)b

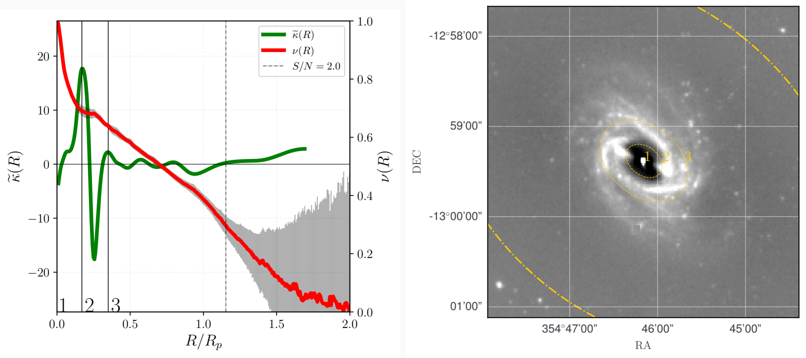

Figure 8: NGC 7723

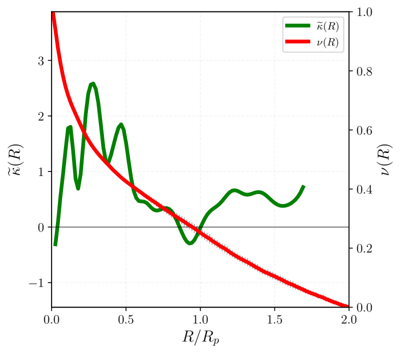

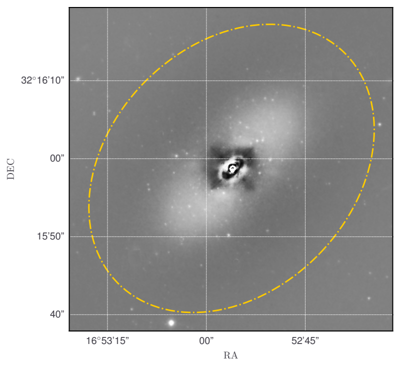

Figure 9: NGC 384

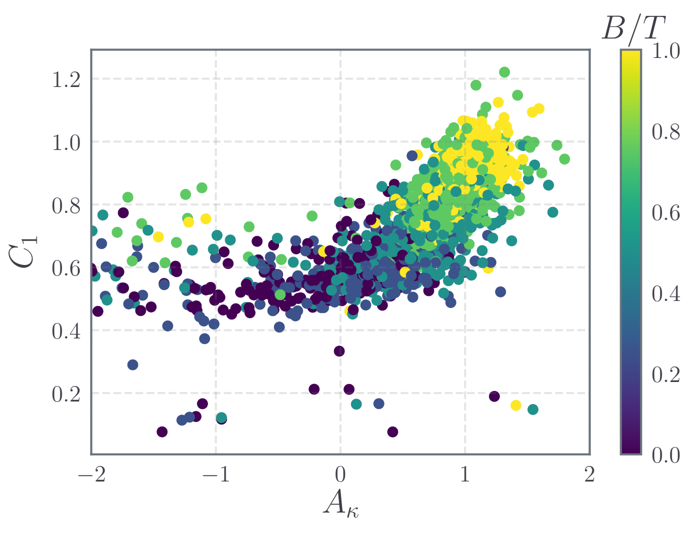

Figure 10: Dada from EFIGI (Baillard et al., 2011).

Curvature Area vs. Information Entropy

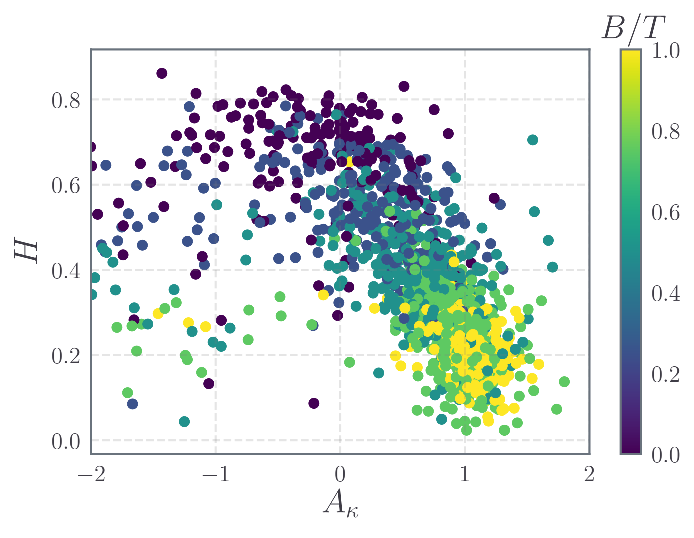

Figure 11: Dada from EFIGI (Baillard et al., 2011).

Conclusions and next steps

Conclusions

- rings and bars have negative curvature/ or are related to high gradient valleys between two local peaks;
- spiral arms makes $\widetilde{\varkappa}$ to oscillate with constant amplitude;
- small values of $\widetilde{\varkappa}$ in the innermost regions might indicate pseudo bulges;
- in the majority of cases, local peaks in $\widetilde{\varkappa}$ are associated to transition regions.

Future work: curvature

- improve the calculation of curvature:
  - optimize $\sigma_{\min}$ and $\sigma_{\max}$: include a explicit dependence on the S/N values;
  - implement an algorithm that detects the local peaks and validate them if they are physically connected to transition regions;
  - furthermore, differentiate valleys associated to bars and rings, if possible;
  - use two-dimensional curvature for further analysis;
- work with a large data set;

Future work: Misclassification of Spirals/Sos

- the concentration index C can leads to misclassification of spiral galaxies (in general, multicomponent galaxies);
- high Sérsic indexes may be related to multicomponent galaxies: smooth secondary components can increase significantly the fitted Sérsic index and leads to misinterpretations;

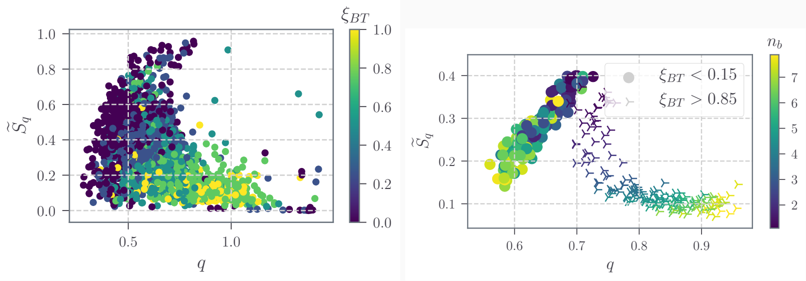

Figure 12: Tsallis entropy S_q.

Questions?

Gracie!

References

Abraham, R. G., Valdes, F., Yee, H. K. C., and van den Bergh, S. (1994). The morphologies of distant galaxies. 1: an automated classification system. *The Astrophysical Journal*, 432:75–90.

Argyle, J. J., Méndez-Abreu, J., Wild, V., and Mortlock, D. J. (2018). Bayesian bulge-disc decomposition of galaxy images. *ArXiv e-prints*.

Baillard, A., Bertin, E., de Lapparent, V., Fouqué, P., Arnouts, S., Mellier, Y., Pelló, R., Leborgne, J.-F., Prugniel, P., Makarov, D., Makarova, L., McCracken, H. J., Bijaoui, A., and Tasca, L. (2011). The EFIGI catalogue of 4458 nearby galaxies with detailed morphology. *Astronomy & Astrophysics*, 532:A74.

Bershady, M. A., Jangren, A., and Conselice, C. J. (2000). Structural and Photometric Classification of Galaxies. I. Calibration Based on a Nearby Galaxy Sample. *The Astronomical Journal*, 119:2645–2663.

Cabrera-Lavers, A. and Garzón, F. (2004). An optical study of a sample of spiral galaxies. *The Astronomical Journal*, 127(3):1386.

Caon, N., Capaccioli, M., and D'Onofrio, M. (1993). On the Shape of the Light Profiles of Early Type Galaxies. *Monthly Notices of the Royal Astronomical Society*, 265:1013.

Conselice, C. J., Bershady, M. A., and Jangren, A. (2000). The Asymmetry of Galaxies: Physical Morphology for Nearby and High-Redshift Galaxies. *The Astrophysical Journal*, 529:886–910.

Crane, K., de Goes, F., Desbrun, M., and Schröder, P. (2013). Digital geometry processing with discrete exterior calculus. In *ACM SIGGRAPH 2013 Courses*, SIGGRAPH '13, pages 7:1–7:126, New York, NY, USA. ACM.

de Souza, R. E., Gadotti, D. A., and dos Anjos, S. (2004). BUDDA: A New Two-dimensional Bulge/Disk Decomposition Code for Detailed Structural Analysis of Galaxies. *The Astrophysical Journal Supplement Series*, 153:411–427.

Erwin, P. (2015). IMFIT: A Fast, Flexible New Program for Astronomical Image Fitting. *The Astrophysical Journal*, 799:226.

Erwin, P. and Sparke, L. S. (2003). An Imaging Survey of Early-Type Barred Galaxies. *The Astrophysical Journal Supplement Series*, 146:299–352.

Ferrari, F., de Carvalho, R. R., and Trevisan, M. (2015). Morfometryka – A New Way of Establishing Morphological Classification of Galaxies. *The Astrophysical Journal*, 814:55.

Gadotti, D. A. (2008). Image decomposition of barred galaxies and AGN hosts. *Monthly Notices of the Royal Astronomical Society*, 384:420–439.

Gadotti, D. A., Athanassoula, E., Carrasco, L., Bosma, A., de Souza, R. E., and Recillas, E. (2007). Near-infrared surface photometry of a sample of barred galaxies. *Monthly Notices of the Royal Astronomical Society*, 381:943–961.

Jungwiert, B., Combes, F., and Axon, D. J. (1997). Near-IR photometry of disk galaxies: Search for nuclear isophotal twist and double bars. *Astronomy & Astrophysics Supplement series*, 125:479–496.

Kent, S. M. (1985). CCD surface photometry of field Galaxies. II - Bulge/disk decompositions. *Astrophysical Journal Supplement Series*, 59:115–159.

Laurikainen, E., Salo, H., and Buta, R. (2005). Multicomponent decompositions for a sample of S0 galaxies. *Monthly Notices of the Royal Astronomical Society*, 362:1319–1347.

Peng, C. Y., Ho, L. C., Impey, C. D., and Rix, H.-W. (2002). Detailed Structural Decomposition of Galaxy Images. *The Astronomical Journal*, 124:266–293.

Peng, C. Y., Ho, L. C., Impey, C. D., and Rix, H.-W. (2010). Detailed Decomposition of Galaxy Images. II. Beyond Axisymmetric Models. *The Astronomical Journal*, 139:2097–2129.

Sérsic, J. L. (1968). *Atlas de galaxias australes*.

Simard, L., Mendel, J. T., Patton, D. R., Ellison, S. L., and McConnachie, A. W. (2011). A Catalog of Bulge+disk Decompositions and Updated Photometry for 1.12 Million Galaxies in the Sloan Digital Sky Survey. *The Astrophysical Journal Supplement*, 196:11.

Sérsic, J. L. (1963). Influence of the atmospheric and instrumental dispersion on the brightness distribution in a galaxy. *Boletin de la Asociacion Argentina de Astronomia La Plata Argentina*, 6:41.

Tenenblat, K. (2008). *Introdução à geometria diferencial*. Edgard Blucher, 2nd edition.

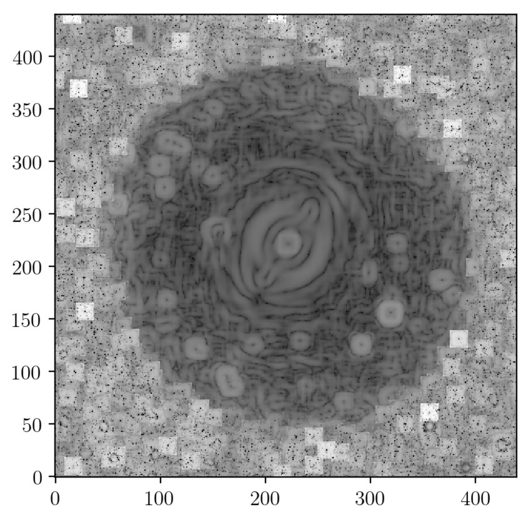

Figure 13: $\widetilde{\varkappa}$ 2D for NGC 1211$-r$.

Additional Material: mfmtk